XMCD and TEM studies of as-cast and rapidly quenched Fe50Nd50 alloys

V. P. Menushenkov, A. P. Menushenkov, I. V. Shchetinin, F. Wilhelm, A. A. Ivanov, I. A. Rudnev, V. G. Ivanov, A. Rogalev, A. G. Savchenko, D. G. Zhukov, et al.

XMCD and TEM studies of as-cast and rapidly quenched $Fe_{50}Nd_{50}$ alloys

IOP Conf. Series: Journal of Physics: Conf. Series **941** (2017) 012072 doi:10.1088/1742-6596/941/1/012072

XMCD and TEM studies of as-cast and rapidly quenched $Fe_{50}Nd_{50}$ alloys

V P Menushenkov[1,*], A P Menushenkov[2], I V Shchetinin[1], F. Wilhelm[3], A A Ivanov[2], I A Rudnev[2], V G Ivanov[2], A Rogalev[3], A G Savchenko[1], D G Zhukov[1], A V Rafalskiy[1], S V Ketov[4]

[1]National University of Science and Technology "MISiS" 119049 Moscow, Russia
[2]National Research Nuclear University MEPhI (Moscow Engineering Physics Institute), Kashirskoe sh. 31, 115409 Moscow, Russia
[3]European Synchrotron Radiation Facility (ESRF), CS40220, F-38043 Grenoble Cedex 9, France
[4] WPI-Advanced Institute for Materials Research, Tohoku University, 2-1-1 Katahira, Aoba-ku, Sendai, 980-8577 Japan

[*]E-mail: menushenkov@gmail.com

Abstract. We present the XMCD analysis of as-cast and melt spun $Fe_{50}Nd_{50}$ samples performed at $L_{2,3}$-Nd and *K*-Fe absorption edges at 5 and 50 K in comparison with macroscopic data of XRD, TEM and magnetic properties measurements. In addition, we have measured the magnetic field dependence of XMCD signal for both types of the samples in magnetic fields up/down to 17 T. The obtained results pointed to the strong difference between structure and magnetic properties of the as-cast and melt spun $Fe_{50}Nd_{50}$ alloys for both macroscopic and local measurements. The element selective XMCD loops for melt spun alloy show almost identical value of the coercive force H_{ci} for L_2-Nd and *K*-Fe edges and practically do not depend on temperature. XMCD loop at *K*-Fe edge is a sum of contributions of the Fe-based phases. The main Fe-rich phase has high $H_{ci} \approx 2{,}4$ T as a highly anisotropic phase. The absence of the *K*-Fe XMCD loop saturation in the field up to 17 T points to presence of the second Nd-rich Nd-Fe phase which is ferromagnetic at temperature lower than 50 K. In accordance to the TEM results these both phases may coexist as the mixture of nanocrystals which was formed as a result of decomposition of the amorphous-like matrix phase. The XMCD loop at L_2-Nd edge with $H_{ci} \approx 1{,}9$ T is the sum of contributions from two Nd-based phases: hard Fe-rich phase ($H_{ci} \approx 2{,}4$ T) and Nd-Fe matrix phase of medium hardness with $H_{ci} \approx 1{,}3$ T. The macroscopic loop showed the higher H_{ci} compared to XMCD loops. Such discrepancy may be caused by the fact that XMCD signal is collected from a 5-10 mcm thick surface layer, which contains many defects that reduce anisotropy and coercivity.

1. Introduction

The interest in the study of the Fe-Nd alloys was renewed during last decade owing to the important role of the Nd-rich intergranular phase in the formation of high coercivity in the sintered Nd-Fe-B-based magnets. The effect of cooling rate and composition on the magnetic properties and microstructure of the melt-spun Nd-Fe alloys was thoroughly investigated. High coercivity values in as-cast Nd-rich Fe-Nd alloys were found to correlate to a metastable eutectic microstructure which includes hard

magnetic phase (A_x) with unidentified structure and composition [1-5]. The formation mechanism of hard magnetic phase during cooling of the Fe-Nd alloys and the structure-property relationship remain unknown. The study of magnetization of the Fe-Nd alloys is complicated due to the presence of several magnetic phases observed by SEM and TEM: primary Nd or Nd_2Fe_{17} phase, Nd and hard magnetic phase as part of eutectic structure. X-ray magnetic circular dichroism (XMCD) technique gives possibility to separate the contribution of Nd and Fe-Nd phases in magnetic behavior of the Fe-Nd alloys. Therefore, the aim of presented study was to characterize the magnetic phases in as-cast and rapidly quenched $Fe_{50}Nd_{50}$ alloys by XMCD and to distinguish their contribution in magnetization process of these alloys.

2. Experimental

The ingot of $Fe_{50}Nd_{50}$ alloy was prepared be melting pure metals in an argon-arc furnace. The rapidly quenched ribbons were made by melt-spinning on a copper-wheel speeded with $v \sim 40$ m·s^{-1} velocity. X-ray diffraction (XRD) studies were carried out using the diffractometer Rigaku Ultima-IV with a graphite monochromator focusing $Co_{K\alpha}$-radiation beam in the Bragg-Brentano geometry. The grain size in the micro- and nanostructure phases of the as-cast and melt spun $Fe_{50}Nd_{50}$ alloys was determined by the JEOL JSM-6610LV scanning electron microscope (SEM) and the JEM-1400 transmission electron microscope (TEM) operated a 120 kV. Measurements of magnetic properties were performed using the physical property measurement system PPMS (EverCoolII, Quantum Design) in fields up to 9 T.

The XMCD studies were carried out at the beamline ID 12 [6] of the European Synchrotron Radiation Facility (ESRF), Grenoble, France. The high-field XMCD end-station was equipped with superconducting solenoid NbTi/Nb_3Sn of Cryogenic Ltd producing a magnetic field up to 17 T in wide temperature range (5 - 300 K). The solenoid axis is set parallel to the incoming X-ray beam. The disks of as-cast or melt spun $Fe_{50}Nd_{50}$ alloy were inserted in a bore of superconducting solenoid so that the disk plane was perpendicular to the solenoid axis. X-ray absorption (XANES) spectra were recorded at the *K*-Fe (7113 eV) and the L_2-Nd (6725 eV) edges in the total fluorescence yield detection mode using Si photodiode mounted on the nitrogen screen of the liquid helium cryostat with solenoid. The APPLE-II type undulator ($h\nu \geq 5$keV) was a source of circularly polarized X-rays and allowed to easily change the polarization of the beam. The XMCD spectra were obtained as a direct difference between consecutive XANES recorded with opposite helicities of the incoming X-ray beam. To ensure that the XMCD spectra are free from any experimental artifacts the data were collected for both directions of the applied magnetic field of 17 T (parallel and antiparallel to the X-ray beam).

In addition, we have measured magnetic field dependence of XMCD signal of as-cast and melt spun $Fe_{50}Nd_{50}$ samples in magnetic fields up/down to 17 T. For that purpose the energy of X-ray monochromator was tuned to the positions of the main maxima of previously recorded XMCD spectra at either Fe *K*- or Nd- absorption edges as in [7,8]. These so-called element selective magnetization curves were compared with macroscopic ones that have measured in the temperature range from 5 to 650 K using a PPMS EverCool-II magnetometer in magnetizing field up to 9 T.

3. Results and discussion

Figure 1 demonstrates the X-ray diffraction patterns for the as-cast and melt spun $Fe_{50}Nd_{50}$ alloy. The XRD pattern of as-cast sample can be indexed by 40% Nd (P63/mmc) and 60% Nd_2Fe_{17} (R-3m).

Figure 1 b shows that the diffraction peaks in the spectra of the ribbon sample are broadened and amorphous background takes place, which should be the result of structural refinement and partial amorphization during melt spinning. The SEM images of the as-cast and melt spun $Fe_{50}Nd_{50}$ alloy are presented in Figure 2. The microstructure of the as-cast sample consists of the primary Nd_2Fe_{17} particles surrounded by the Nd-rich cover with eutectic region between them (left panel). At the same time, the SEM image of the ribbon sample shows a single-phase homogeneous microstructure (right panel).

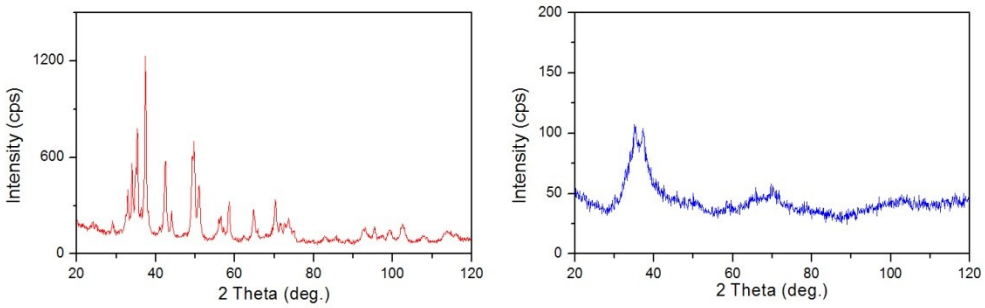

Figure 1. XRD patterns for the as-cast and melt spun $Fe_{50}Nd_{50}$ alloys

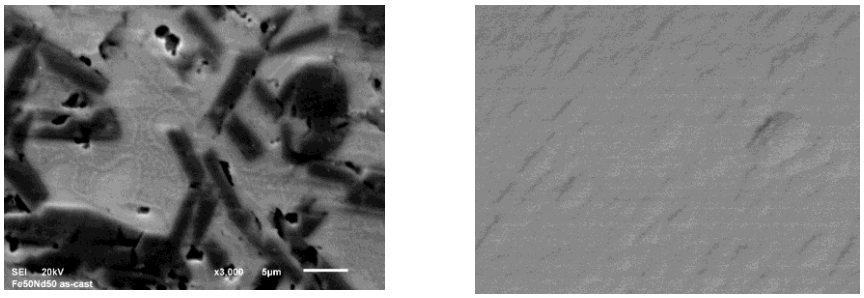

Figure 2. SEM micrographs of the as-cast and melt spun $Fe_{50}Nd_{50}$ samples

The hysteresis loops for the as-cast and melt spun $Fe_{50}Nd_{50}$ alloys are shown in Figure 3. The very low coercive force of the as-cast sample results from the high-volume fraction of the soft Nd_2Fe_{17} phase at all measured temperatures. However, the visible width of the loops at high magnetic fields at temperature lower than 50 K points to the presence of the hard magnetic phase in the microstructure of as-cast alloy, and also to the presence of the Nd-based phase which is not saturated up to 17 T. Measurements of the melt spun $Fe_{50}Nd_{50}$ ribbon showed the kink in the low demagnetization field. This fact is evidence that some part of the sample volume is magnetically soft, which can arise from the presence of a soft magnetic phase Nd_2Fe_{17} in the melt spun ribbon.

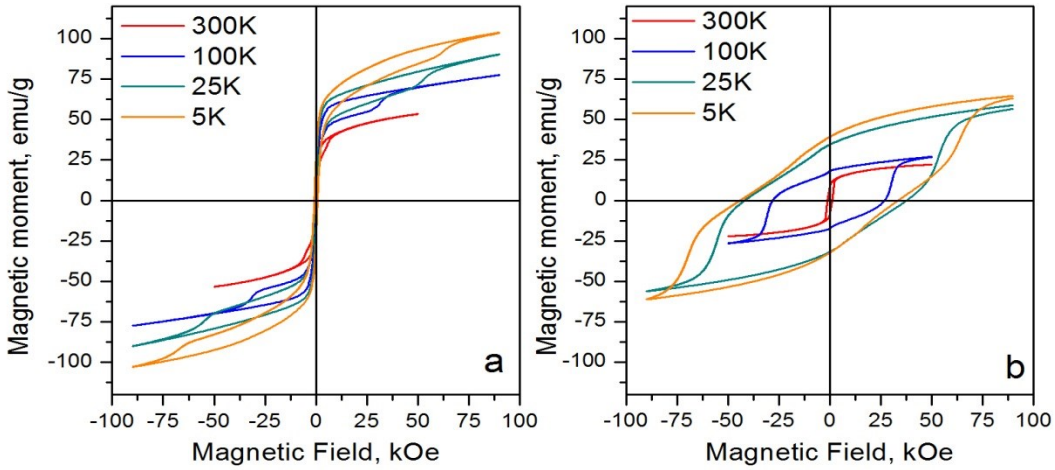

Figure 3. Hysteresis loops for the as-cast and melt spun $Fe_{50}Nd_{50}$ samples at 5 - 300 K

The dark field images of the ribbon $Fe_{50}Nd_{50}$ are presented in Figure 4(a). The microstructure of the ribbon consists of amorphous-like regions with nanocrystals of the unknown phases. The darkfield image of the Nd-Fe region taken in the nearest ring reflection of the selected area electron diffraction (SAED) pattern is shown in Figure 4. This image indicates that the Fe-Nd region is composed of a fine dispersed phase with 5–10 nm in diameter and of an amorphous-like phase.

XMCD spectra recorded at $L_{2,3}$-Nd and *K*-Fe absorption edges for the ribbon $Fe_{50}Nd_{50}$ alloy are presented in Figure 5 together with corresponding normalized X-ray absorption (XANES) spectra. It has been shown [4,5] that the first feature (minimum) in the XMCD spectrum at the L_3 absorption edge of Nd is due to $2p_{3/2} \rightarrow 4f_{5/2}$ quadrupole transitions, whereas the second one (major maximum) corresponds to dipole transitions $2p_{3/2} \rightarrow 5d_{3/2,5/2}$. The XMCD signal of the L_2-Nd-absorption edge has a pronounced major maximum, corresponding to dipole transitions $2p_{1/2} \rightarrow 5d_{3/2}$ and a very weak negative feature at lower photon energies that could be attributed to quadrupole transitions. The observed spectra at the *K*-Fe -edge are due to dipole transitions from 1*s* core level of Fe to 4*p* states in the conduction band that are hybridized with the 3*d* states of iron. The *K*-Fe edge XMCD signal is much smaller in comparison with $L_{2,3}$-Nd edge XMCD signal because of low magnetization of the 4*p* states.

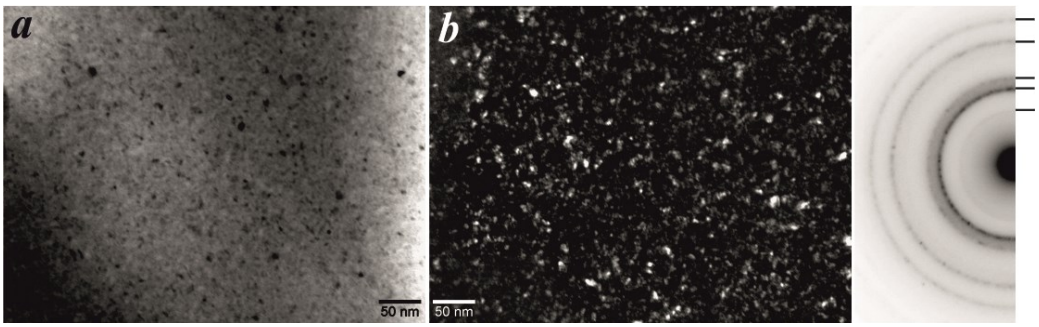

Figure 4. Bright-field (*a*) and dark-field (*b*) images of the ribbon x = 50 sample taken in the second ring reflection of the SAED pattern

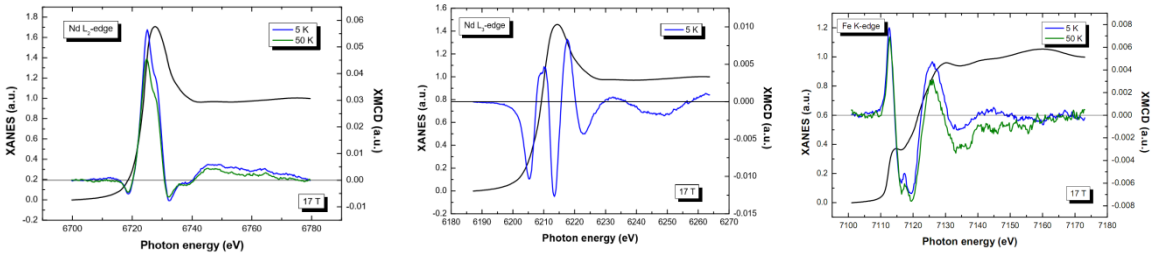

a) b) c)

Figure 5. Comparison of XANES and XMCD spectra measured at $L_{2,3}$-Nd (a,b) and Fe-*K* (c) edges of melt spun $Fe_{50}Nd_{50}$ alloy in the magnetic field H = 17 T at 5 and 50 K

In addition to XMCD spectra at the L_2-Nd and at the *K*-Fe edges, we have measured so-called XMCD magnetization curves that are shown in Figure 6. These element-selective magnetization curves have been recorded at temperatures 5 and 50 K in fields up/down to 17 T by monitoring the magnitude of XMCD signal at the photon energy corresponding to a major maximum as a function of an applied magnetic field. For the case of L_2-Nd absorption edges the measurements were performed at the positions of first maximum 6.725 keV, while for *K*-Fe -edge the major maximum of XMCD spectra was observed at 7.113 keV. These measurements are fundamentally different from the conven-

tional macroscopic magnetization curves measurements, which give information about the integrated characteristics of the magnetization reversal.

Figure 6 shows the XMCD magnetic loops measured at L_2-Nd and K-Fe edges at 5 and 50 K, respectively. One can see that XMCD loops for L_2-Nd and K-Fe edges show almost identical value of the coercive force and are practically independent of temperature. The element selective XMCD loops were compared with macroscopic ones measured using a magnetometer at 5 K (Figure 7).

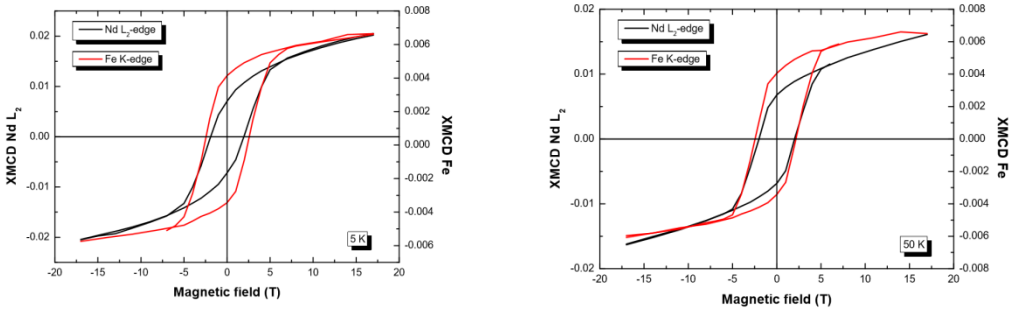

Figure 6. XMCD hysteresis loops measured at L_2 -Nd and K-Fe edges for ribbon $Fe_{50}Nd_{50}$ at 5 K (left panel) and 50 K (right panel)

The XMCD loop at K-Fe edge is a sum of contributions of the Fe-based phases. The main Fe-rich phase has high $H_{ci} \approx 2{,}4$ T (Figure 7) hence it is a highly anisotropic phase. Since the XMCD loop at K-Fe edge is not saturated in the field up to 17 T there exists the second Nd-rich Nd-Fe phase which is ferromagnetic at temperature lower than 50 K.

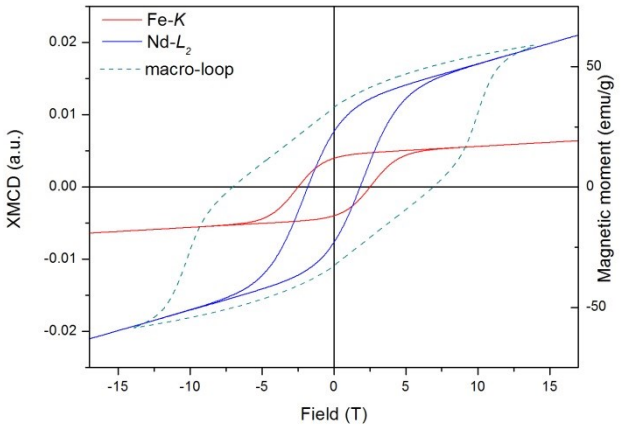

Figure 7. Macroscopic hysteresis loop for as-cast $Fe_{50}Nd_{50}$ sample in comparison with HMCD hysteresis loops, measured on L_2-Nd and K-Fe edges at 5 K

According to the TEM results (Figure 4) both phases (A_x and Nd-rich) may coexist as the mixture of nanocrystals which was formed because of decomposition of the amorphous-like matrix phase. The XMCD loop at L_2-Nd edge with $H_{ci} \approx 1{,}9$ T is resulted from contributions of the Nd-based phases: these include hard A_x phase ($H_{ci} \approx 2{,}4$ T) and medium hard Nd-Fe phase with $H_{ci} \approx 1{,}3$ T. Presumably, in the ribbon $Fe_{50}Nd_{50}$ the last phase can be a matrix.

It worth noticing that the macroscopic loop in the Figure 7 normalized to the saturation of the XMCD L_2-Nd loop showed a higher coercive force ($H_{ci} = 4{,}7$ T) compared to XMCD loop ($H_{ci} \approx 1{,}9$ T). At the same time, as can be seen in Figures 3 and 7, the coupling of both macroscopic and

XMCD L_2-Nd hysteresis loops occurs in a field of about 7,5 T which is higher than coercive force. Therefore, this value of field should be used to compare the difficulty of the magnetization reversal process. The reason of the difference between values of H_{ci} may be that macroscopic loop results from remagnetization of the bulk of alloy while the XMCD loop is obtained from a 5-10 mcm thick surface layer. The surface contains many defects that may reduce anisotropy and coercivity. Indeed, both the coercivity of XMCD loop and penetration depth of X-ray at *K*-Fe edge (7113 eV) are bigger than corresponding quantities at L_2-Nd edge (6725 eV).

4. Conclusion

XMCD analysis of as-cast and melt spun $Fe_{50}Nd_{50}$ samples was performed at $L_{2,3}$-Nd and *K*-Fe absorption edges at 5 and 50 K. In addition, we have measured the magnetic field dependence of XMCD signal for both types of samples in magnetic fields up/down to 17 T. This element-specific information was compared with the macroscopic magnetic and structure properties of the same samples measured by XRD, SEM, TEM and PPMS EverCool-II magnetometer. The obtained results pointed to the strong difference between structure and magnetic properties of the as-cast and melt spun $Fe_{50}Nd_{50}$ alloys for both macroscopic and local measurements. The XRD pattern of as-cast sample was indexed as 40% Nd (P63/mmc) and 60% Nd_2Fe_{17} (R-3m) phases, while for ribbon samples the diffraction peaks are broadened and amorphous background take place as a result of structural refinement and partlial amorphization during melt spinning. The TEM images show that the microstructure of the as-cast sample consists of the primary Nd_2Fe_{17} particles surrounded by the Nd-rich cover with eutectic region between them, while the ribbon sample has a single-phase homogeneous microstructure. The element selective XMCD loops for melt spun alloy show the almost identical value of the coercive force for L_2-Nd and *K*-Fe edges and practically don't depend from temperature. XMCD loop at *K*-Fe edge is a sum of contributions of the Fe-based phases. The main Fe-rich phase has high $H_{ci} \approx 2{,}4$ T as a highly anisotropic phase. The absence of the *K*-Fe XMCD loop saturation in the field up to 17 T points to presence of the second Nd-rich Nd-Fe phase which is ferromagnetic at lower than 50 K temperature. According to the SEM results both phases may coexist as the mixture of nanocrystals which was formed as a result of decomposition of the amorphous-like matrix phase. The XMCD loop at L_2-Nd edge with $H_{ci} \approx 1{,}9$ T is the sum of contributions from two Nd-based phases: hard Fe-rich phase ($H_{ci} \approx 2{,}4$ T) and Nd-Fe matrix phase of medium hardness with $H_{ci} \approx 1{,}3$ T. The macroscopic loop normalized to the saturation point of the XMCD L_2-Nd loop showed a higher H_{ci} compared to XMCD loops, since the XMCD loop is obtained from a thin surface layer of 5-10 mcm thickness, which may contain many defects that reduce anisotropy and coercivity.

Acknowledgements

The authors acknowledge the ESRF Program Committee for providing the opportunity of XMCD measurements at ID12 beamline in according with MA-3314 project. This work was supported by the Ministry of Education and Science of the Russian Federation (agreement no. 14.587.21.0028, unique number of project RFMEFI58716X0028).

References

[1] Delamare J, Lemarch D, P. Vigier P 1994 *J. Alloys Compd.* **216** 273
[2] Menushenkov V P, Anderson S J, and Hoier R 1998 Proc. of the 20-th Int. Symp. on Magnetic Anisotropy and Coercivity in Rare-Earth Transition Metal Alloys, ed. By L. Schultz and K.-H. Müller, Werkstoff-Infromationsgesellschaft, Frankfurt, p. 97
[3] Menushenkov V P, *et al* 1999 *J. Magn. Magn. Mater.* **203** 149
[4] Kumar G, J. Eckert J, Roth S, Löser W, Schultz L and Ram S2003 *Acta Mater.* **51** 229
[5] Kumar G, Filip O, Löser W, Schultz L, Eckert J 2006 *Intermetallisc* **14** 47
[6] Sarafidis C, Wilhelm F, Rogalev A, *et al* 2009 *J. Phys.: Condens. Matter***21** 236001
[7] Menushenkov A P, Ivanov V G, Shchetinin I V, *et al* 2017 *JETP Letters* **105** 38
[8] Menushenkov A P, Ivanov V G, Shchetinin I V, *et al* 2016 *J. Phys.: Conf. Ser* **747** 012039